Calcium regulates tertiary structure and enzymatic activity of human endometase/matrilysin-2 and its role in promoting human breast cancer cell invasion

Seakwoo LEE, Hyun I. PARK and Qing-Xiang Amy SANG[1]

Department of Chemistry and Biochemistry and Institute of Molecular Biophysics, Florida State University, Tallahassee, FL 32306-4390, U.S.A.

Human MMP-26 (matrix metalloproteinase-26) (also known as endometase or matrilysin-2) is a putative biomarker for human carcinomas of breast, prostate and other cancers of epithelial origin. Calcium modulates protein structure and function and may act as a molecular signal or switch in cells. The relationship between MMPs and calcium has barely been studied and is absent for MMP-26. We have investigated the calcium-binding sites and the role of calcium in MMP-26. MMP-26 has one high-affinity and one low-affinity calcium binding site. High-affinity calcium binding was restored at physiologically low calcium conditions with a calcium-dissociation constant of 63 nM without inducing secondary and tertiary structural changes. High-affinity calcium binding protects MMP-26 against thermal denaturation. Mutants of this site (D165A or E191A) lose enzymatic activity. Low-affinity calcium binding was restored at relatively high calcium concentrations and showed a K_{d2} (low-affinity calcium-dissociation constant) value of 120 μM, which was accompanied with the recovery of enzymatic activity reversibly and tertiary structural changes, but without secondary structural rearrangements. Mutations at the low-affinity calcium-binding site (C3 site), K189E or D114A, induced enhanced affinity for the Ca^{2+} ion or an irreversible loss of enzymatic activity triggered by low-affinity calcium binding respectively. Mutation at non-calcium-binding site (V184D at C2 site) showed that C2 is not a true calcium-binding site. Observations from homology-modelled mutant structures correlated with these experimental results. A human breast cancer cell line, MDA-MB-231, transfected with wild-type MMP-26 cDNA showed a calcium-dependent invasive potential when compared with controls that were transfected with an inactive form of MMP-26 (E209A). Calcium-independent high invasiveness was observed in the K189E mutant MDA-MB-231 cell line.

Key words: breast cancer cell invasion, calcium, endometase, matrilysin-2, matrix metalloproteinase 26 (MMP-26).

INTRODUCTION

MMPs (matrix metalloproteinases) are a family of proteolytic enzymes that degrade components of the ECM (extracellular matrix) such as collagen, gelatin, fibronectin, vitronectin and laminin [1,2]. MMPs are known to participate in reproduction, angiogenesis, development, morphogenesis and tissue remodelling, as well as pathological conditions, including arthritis, cardiovascular disease, and cancer progression and metastasis [1–3]. MMP-26 (also known as endometase/matrilysin-2) is the smallest member of the MMP family, comprising only pro- and catalytic domains like MMP-7 (matrilysin), but without a haemopexin-like domain [4–7]. According to peptide library screening and kinetic studies, MMP-26 has a substrate specificity similar to that of other MMPs, such as MMP-2 and MMP-9 [8]. MMP-26 promotes the invasion of a highly metastatic and tumorigenic prostate cancer cell line through its activation of pro-MMP-9 (pro-gelatinase B) [9]. Expression level of MMP-26 is significantly higher in pre-invasive human breast DCIS (ductal carcinoma *in situ*) [10,11] and HGPIN (high-grade prostatic intraepithelial neoplasia) [12] compared with that in normal human breast tissue samples and non-neoplastic ducts. Level of MMP-26 expression is also high in early stages (I and II) of invasive carcinoma, whereas in stage III invasive carcinomas the level of MMP-26 decreases [10,12]. This is similar to the discovery that a high level of MMP-26 expression was detected in low-grade SCC (squamous cell cancer), but not in dedifferentiated grade III tumours [13]. Thus MMP-26 could be a marker of early-stage cancer [10–13].

Ca^{2+} ions have numerous critical roles in biological systems with involvement in cell-cycle regulation, proliferation, cell migration, angiogenesis and apoptosis, with enzymes such as calmodulin, calbindin and calpain [14–20]. Ca^{2+} ions also participate as signalling mediators in biological systems [21]. Ca^{2+} ions regulate divergent calcium cascade pathways in cancer cells compared with normal cells, as a result of differing protein expression patterns in these cells [22]. For example, cancer cells respond to hormones via Ca^{2+}-regulatory mechanisms that result in Ca^{2+}-mediated apoptosis, whereas normal cells do not [18]. Normally, very low Ca^{2+} ion concentrations are maintained in the cytoplasm (300–1200 nM) [23]. When the cell is activated by an extracellular signal, Ca^{2+} ions are released from the endoplasmic reticulum or enter through voltage-gated Ca^{2+} channels in the cell membrane, resulting in cytosolic calcium concentrations of approx. 5 μM [23]. This fluctuation of calcium concentrations can alter cellular physiology by means of structural changes induced by calcium-binding proteins, such as the calcium-mediated electrostatic switch mechanism for m-calpain [24]. Binding of Ca^{2+} ions to proteins may confer structural stability in which reagent-induced and thermal denaturation [25,26] are less probable, or modulate substrate binding [27].

On the basis of crystallographic studies of the catalytic domains of fibroblast collagenase/MMP-1 [28], stromelysin-1/MMP-3 [29], matrilysin/MMP-7 [30], neutrophil collagenase/MMP-8 [31], stromelysin-3/MMP-11 [32], macrophage metalloelastase/MMP-12 [33] collagenase-3/MMP-13 [34] and MT1-MMP (membrane-type-1 MMP) [35], at least two calcium-binding

Abbreviations used: ANS, 8-anilino-1-naphthalenesulfonate; DMEM, Dulbecco's modified Eagle's medium; ECM, extracellular matrix; FBS, fetal bovine serum; LACD, low-affinity-Ca^{2+}-ion-depleted; MMP, matrix metalloproteinase; MT1-MMP, membrane-type-1 MMP; Quin2, 2-({2-[bis(carboxymethyl)amino]-5-methylphenoxy}methyl)-6-methoxy-8-[bis(carboxymethyl)amino]quinoline; RMSD, root mean square deviation.

[1] To whom correspondence should be addressed (email sang@chem.fsu.edu).

Table 1 Primers used for mutagenesis

Mutant	Primer	Sequence
D114A	Forward	5′-CAATTACCCACATGCTATGAAGCCATCCG-3′
	Reverse	5′-CGGATGGCTTCATAGCATGTGGGTAATTG-3′
D165A	Forward	5′-GATGGTTGGCCCTTTGCTGGGCCAGGTGGTATC-3′
	Reverse	5′-GATACCACCTGGCCCAGCAAAGGGCCAACCATC-3′
V184D	Forward	5′-GGAAATCCTGGAGATGTCCATTTTGAC-3′
	Reverse	5′-GTCAAAATGGACATCTCCAGGATTTCC-3′
K189E	Forward	5′-GTTGTCCATTTTGACGAGAATGAACACTGG-3′
	Reverse	5′-CCAGTGTTCATTCTCGTCAAAATGGACAAC-3′
E191A	Forward	5′-CCATTTTGACAAGAATGCACACTGGTCAGCTTCAG-3′
	Reverse	5′-CTGAAGCTGACCAGTGTGCATTCTTGTCAAAATGG-3′
E209A	Forward	5′-CCTGGTTGCAACTCATGCGATTGGGCATTCTTTGG-3′
	Reverse	5′-CCAAAGAATGCCCAATCGCATGAGTTGCAACCAGG-3′

sites have been identified. Previous studies have shown that Ca^{2+} ions stabilize MMP-1 [25], mediate signal transduction in the expression of MMP-2 [36], facilitate the activation of pro-MMP-3 [37], and induce cleavage of both N- and C-termini, resulting in activation and C-terminal truncation of pro-MMP-9 from the complex of pro-MMP-9 and chondroitin sulfate proteoglycans [38], and that Ca^{2+} ion influx inhibits MT1-MMP processing [39]. However, little research has focused on the structural and functional roles of Ca^{2+} ions in MMPs. We have recently observed that Ca^{2+} ions can modulate the catalytic activity of MMP-26 through conformational changes in the active site. We investigated the characteristics of calcium binding in wild-type and mutant forms of MMP-26 by means of calcium titration monitoring fluorescent peptide hydrolysis, by fluorescence spectroscopy with ANS (8-anilino-1-naphthalenesulfonate) and Quin2 [2-({2-[bis(carboxymethyl)amino]-5-methylphenoxy}methyl)-6-methoxy-8-[bis-(carboxymethyl)amino]quinoline] and CD spectroscopy. Cellular invasion assays lend additional support to the consequential role of Ca^{2+} ions in enzymatic function. In the present study we investigated the characteristics of calcium binding in MMP-26.

MATERIALS AND METHODS

Construction of pro-MMP-26 and mutant forms

Human endometase was cloned and ligated into pET-20b(+) and subsequently expressed in *Escherichia coli* as described previously [4]. cDNA of pro-MMP-26 was amplified by PCR using forward primer, containing a HindIII restriction site (underlined), 5′-CCCAAGCTTGTTCCAGTGCCCCCTGCTGCAGACCAT-3′ and reverse primer, containing a BglII restriction site (underlined), 5′-GAAGATCTAGGTATGTCAGATGAA- CATTTTTCTCC-3′, and subcloned into the pFLAG-CTS expression vector (Sigma) between the HindIII and BglII sites. In order for cDNA to be aligned with the ATG translational start codon, an extra nucleotide following the OmpA Signal Peptide (signal sequence for secretion of C-terminal FLAG fusion proteins to periplasmic space) was deleted using forward primer, 5′-GCTACCGTTGCGCAAGCTGTTCCAGTGCCCCCTGCT-3′, and reverse primer, 5′-AGCAGGGGGCACTGGAACAGCTTGCGCAACGGTAGC-3′. Site-directed mutagenesis of putative calcium-binding sites, D114A, D165A, V184D, K189E and E191A, and catalytic Glu^{209}, E209A, was accomplished using PCR with the primers given in Table 1. Mutant constructs were transformed into *E. coli* DH5α cells for amplification and purification of the pFLAG-CTS/pro-MMP26 vector. Sequences were confirmed by DNA sequencing using an N-26 sequencing primer (Sigma), 5′-CATCATAACGGTTCTGGCAAATATTC-3′ for pFLAG-CTS/pro-MMP-26. Resulting constructs were transformed into *E. coli* BL21 cells for expression and purification of the protein. cDNA of pro-MMP-26 was also subcloned into the p3xFLAG-CMV™-13 expression vector (Sigma) between the HindIII and XbaI sites. The PCR primer for the 5′ HindIII restriction site was the same as the pFLAG-CTS subcloning primer, and for the XbaI restriction site (underlined), 5′-GCTCTAGAAGGTATGTCAGATGAACATTTTTCTCC-3′. Site-directed mutagenesis of the putative calcium-binding site (K189E) and catalytic Glu^{209} (E209A) was accomplished using PCR with the same primers as above for p-FLAG-CTS. The p3xFLAG-CMV™-13/pro-MMP-26 vector was amplified and purified using the above methods. Sequences were confirmed by DNA sequencing using an N-CMV sequencing primer (Sigma), 5′-AATGTCGTAATAACCCCGCCCCGTTGACGC-3′, for p3xFLAG-CMV™-13/pro-MMP-26.

Expression of MMP-26 in *E. coli* and refolding of the denatured protein

Expression of the catalytic domain of MMP-26, but not its prodomain, caused improper folding and resulted in an inactive enzyme (results not shown). Therefore the prodomain is necessary to chaperone active enzyme formation. The activation mechanism of MMP-26 is still unclear, but is likely to involve auto-activation [8,40]. Active MMP-26 was prepared as described previously [4]. In brief, MMP-26 was expressed in the form of inclusion bodies from *E. coli* BL21 cells. The inclusion bodies were isolated and purified using B-PER™ (Pierce, Rockford, IL) bacterial protein extraction reagent according to the manufacturer's instructions. The insoluble protein was dissolved in 8 M urea and 25 mM Tricine at approx. 2.5 mg/ml and then refolded by dialysis. During dialysis, pro-MMP-26 was auto-activated. Folding and activation patterns were determined by electrophoresis followed by Western blotting with an anti-FLAG M2 monoclonal antibody (Sigma). SeeBlue Plus2 pre-stained standard (Invitrogen) was used to determine the molecular mass of MMP-26. The protein was purified using an anti-FLAG M2 affinity column (Sigma). The enzyme concentration was measured with a molar absorption coefficient, ε_{280}, of 57 130 $M^{-1} \cdot cm^{-1}$ using GCG (Genetics Computer Group) software as described previously [4].

Removal of low-affinity, or both high- and low-affinity, Ca^{2+} ions

Sequence alignment and crystal structural analysis revealed the possibility of both low- and high-affinity calcium-binding sites for MMP-26. To remove the low-affinity Ca^{2+} ions (i.e. Ca^{2+} ions bound to low-affinity binding sites), the enzyme was dialysed three times in 0.01 % Brij-35 (polyoxyethlene dodecyl ether), 10 mM Hepes/NaOH, pH 7.5, 10 mM NaCl and 0.1 μM $ZnSO_4$ for 8 h at 4 °C. This was followed by dialysis in the presence of 0.1 % Chelex 100 (Sigma). The affinity of Chelex 100 for Ca^{2+} ions is not particularly high, with a binding constant of 4.6×10^3 M^{-1}. Therefore this method removed only the low-affinity Ca^{2+} ions from the enzyme [41]. Dialysis in the presence or absence of Chelex 100 did not alter further experiments. Adding Chelex 100 ensured the removal of low-affinity Ca^{2+} ions from the enzyme. To eliminate the high-affinity Ca^{2+} ions (i.e. Ca^{2+} ions bound to high-affinity binding sites), the enzyme was dialysed three times in the presence of 0.01 % Brij-35, 2 mM EGTA, 10 mM Hepes/NaOH, pH 7.5, 0.1 M NaCl and 0.1 μM $ZnSO_4$ for 8 h at 4 °C, followed by dialysis three times in 0.01 % Brij-35, 10 mM Hepes/NaOH, pH 7.5, 10 mM NaCl and 0.1 μM $ZnSO_4$ for 8 h at 4 °C, in order to remove EGTA. For CD spectroscopy,

10 mM Tris/HCl was substituted for 10 mM Hepes/NaOH. For ANS-binding assays, Brij-35 was omitted from the buffer to avoid interactions between ANS and Brij-35.

Fluorescence titration with Quin2

A Quin2 (Sigma) stock solution (approx. 500 μM) was prepared by dissolution in buffer (Chelex 100-treated 10 mM Hepes/NaOH, pH7.5, and 10 mM NaCl). The concentration of the Quin2 stock solution was determined by using the molar absorption coefficient, ε_{240}, of 4.2×10^4 $M^{-1} \cdot cm^{-1}$, following a 1:100 dilution of stock solution in the presence of 10 mM $CaCl_2$ [42]. LACD (low-affinity-Ca^{2+}-ion-depleted) enzymes used for the Quin2 titration experiments were prepared by dialysis as described above. Titration was performed at 25 °C in a quartz cell (1 cm × 0.5 cm). All measurements were performed in 10 mM Hepes/NaOH, pH 7.5, and 10 mM NaCl at 25 °C. Titration was performed by adding 5 μl aliquots of 300 μM Quin2 to 1500 μl of a 2.5 μM enzyme solution in a quartz cell. Time-dependence assays of Quin2 binding to Ca^{2+} showed no change in Quin2 fluorescence after MMP-26 was mixed with a 20-fold excess of Quin2 at 25 °C in 10 mM Hepes buffer, after 5–40 min (results not shown). At each titration point, the sample was incubated for 10 min before measuring the emission spectra from 450 to 530 nm with 5 nm excitation and emission slit width at an excitation wavelength of 339 nm. The emission was scanned at a rate of 2 nm/s. Fluorescence spectra intensity changes of the Quin2–Ca^{2+} complex were monitored at 490 nm. Background fluorescence spectra of Quin-2 were measured by using either water or buffer in the presence of various concentrations of Quin2. Background fluorescence spectra of water and buffer were identical and showed no calcium contamination.

Calculation of the high-affinity calcium-dissociation constant, K_{d1}, following fluorescence titration with Quin2

Calcium-dissociation constants ($K_{dCa^{2+}}$) for proteins can be calculated using several methods [42,43], assuming that the increase in fluorescence intensity is proportional to the concentration of the Quin2–Ca^{2+} complex [44]. In the present study, in the presence of the calcium-binding protein, the apparent dissociation constant of the Quin2–Ca^{2+} complex, $K_{d(QCa)}$, was calculated by fitting experimental data to the following equation [42]:

$$F_i = \frac{f_i}{V - 1} = \frac{[Ca]_T + [Q]_i + K_{d(QCa)} - \sqrt{([Ca]_T + [Q]_i + K_{d(QCa)})^2 - 4[Q]_i[Ca]_T}}{2[Ca]_T} \quad (1)$$

where f_i is the intensity of fluorescence at each point, V is the maximum of the fluorescence, $[Ca]_T$ is the total calcium concentration, and $[Q]_i$ is Quin2 concentrations at each point. $K_{d(QCa)}$ may then be applied to the following equation in order to obtain the high-affinity calcium-dissociation constant of the enzyme, K_{d1}:

$$K_{d1} = K_Q\left(1 + [E]/K_{d(QCa)}\right) \quad (2)$$

where [E] is the enzyme concentration, and K_Q is the calcium-dissociation constant for Quin2 (5.3 nM) at low salt concentrations [43].

Calcium titration by monitoring enzyme activity

The fluorescence-quenched peptide substrate Mca [(7-methylcoumarin-4-yl)acetyl]-Pro-Leu-Gly-Leu-Dap (2,3-diaminopropyl)-Dnp (2,4-dinitrophenyl)-Ala-Arg-NH_2 (Bachem) was used to measure the rate of substrate hydrolysis. Enzyme activity was measured using a PerkinElmer LS 50B Luminescence Spectrometer connected to a constant-temperature water bath at 25 °C. Release of the fluorescent cleavage product was monitored by measuring fluorescence ($\lambda_{excitation} = 328$ nm and $\lambda_{emission} = 393$ nm), where the increase of fluorescence intensity is proportional to substrate hydrolysis. Assays were performed in 0.01 % Brij-35, 10 mM Hepes/NaOH, pH 7.5, and 10 mM NaCl, with various Ca^{2+} concentrations at 25 °C. Different concentrations of Ca^{2+} stock solutions were prepared by serial dilutions from 1.6 M to 20 μM. Enzymes (final concentration of 0.1 μM) were incubated in 0.01 % Brij, 10 mM Hepes/NaOH, pH 7.5, and 10 mM NaCl with varying concentrations of Ca^{2+} solution in a quartz cell (3 mm × 3 mm) for an incubation period of 20 min. Assays commenced with the addition of a substrate stock solution to a final concentration of 1 μM. Calcium reagent (Sigma) contained less than 0.0005 % (w/w) Zn^{2+} ions. The EC_{50} value of Ca^{2+} was 0.12 mM, resulting in less than 0.37 nM of possible Zn^{2+} ion contamination. Denatured MMP-26 from the bacterial extract was refolded in the presence of 0.1 μM Zn^{2+} to produce folded and activated MMP-26. Therefore incubation of LACD-MMP-26 with 0.1 μM Zn^{2+} is an appropriate zinc concentration to restore Zn^{2+} ions, if lost. However, incubation of LACD-MMP-26 with a final concentration of 0.1 μM Zn^{2+} had no effects on enzymatic activity, leading to the conclusion that dialysis did not remove Zn^{2+} ions from enzyme and Zn^{2+} ions were unlikely to have affected the experimental outcomes.

Calculation of the low-affinity calcium-dissociation constant, K_{d2}

If a single Ca^{2+} ion regulates enzymatic activity, then the calcium-dissociation constant, K_{d2}, can be expressed as follows:

$$K_{d2} = [E]_{free}[Ca^{2+}]_{free}/[ECa^{2+}]$$

$$[E]_{Total} = [E]_{free} + [ECa^{2+}]$$

$$[Ca^{2+}]_{Total} = [Ca^{2+}]_{free} + [ECa^{2+}]$$

when enzymatic activity reaches 50 % of the maximum

$$[E]_{free} = [ECa^{2+}]$$

$$[E]_{Total} = 2[ECa^{2+}]$$

Therefore $K_{d2} = [Ca^{2+}]_{Total} - 0.5[E]_{Total}$. If it is assumed that $[Ca^{2+}]_{Total}$ is much greater than $[E]_{Total}$, then $K_{d2} = [Ca^{2+}]_{Total}$ at 50 % enzymatic activity, the EC_{50} value.

For MMP-26, E stands for LACD-MMP-26 and Ca^{2+} stands for the low-affinity Ca^{2+} ion. We assume that the high-affinity Ca^{2+} ion was not dissociated from LACD-MMP-26 owing to its low value of dissociation constant, K_{d1}.

ANS binding

An ANS (Sigma) stock solution of 1 mM was prepared by dissolving ANS in 10 mM Hepes, pH 7.5, and 10 mM NaCl. ANS concentration was determined by using the molar absorption coefficient, ε_{350}, of 5000 $M^{-1} \cdot cm^{-1}$ [45]. LACD-MMP-26 utilized for the ANS-binding experiments were prepared by dialysis as described above in the absence of Brij-35. All measurements were performed in 10 mM Hepes, pH 7.5, and 10 mM NaCl, with various Ca^{2+} concentrations, at 25 °C in a quartz cell (3 mm × 3 mm) after 20 min of incubation. To saturate the hydrophobic sites of the enzyme with ANS, 100 μM ANS was added to 3.4 μM of wild-type MMP-26 or 2 μM of mutant-form MMP-26 solution,

constituting a 30-fold molar excess. ANS emission spectra were obtained from 405 to 560 nm with 5 nm excitation and emission slit widths at an excitation wavelength of 395 nm. Changes in ANS fluorescence spectra, owing to the binding of ANS to protein, were monitored at 480 nm.

CD spectroscopy

CD was used to monitor changes in the secondary structure of the enzyme. Protein samples for CD spectroscopy experiments were prepared by dialysis as described above. All measurements were performed in 10 mM Tris/HCl, pH 7.5, 10 mM NaCl and 0.01 % Brij-35. CD spectra were obtained after the enzyme had been incubated for 2 h in the presence of 2 mM EGTA (400-fold excess) or in 10 mM $CaCl_2$ solution. CD spectroscopic measurements were performed on an Aviv 62 ADS CD spectrometer equipped with a 0.1-cm-pathlength cell and a thermoelectric cuvette holder and connected to a model CFT-33 refrigerated recirculator (NESLAB). CD spectra were acquired by scanning from 260 to 185 nm in 0.5 nm increments with a 1 nm bandwidth. Triplicate scans were recorded, averaged and analysed. Buffer scans were subtracted, and the data were converted into molar ellipticity ($[\theta]$, degrees $\cdot$ cm^2 $\cdot$ dmol^{-1}). Thermal denaturation transitions were measured by continuously monitoring ellipticities at a fixed wavelength of 218 nm while the temperature of the sample was increased. Data were collected at 3 °C increments from 4 °C to 61 °C. The apparent fractional extent of unfolding, f_{app}, was calculated from the molar ellipticity values ($[\theta]$) at 218 nm using the following equation:

$$f_{app} = ([\theta]_N - [\theta])/([\theta]_N - [\theta]_U)$$

where $[\theta]_N$ and $[\theta]_U$ represent ellipticity values of the native and non-native states respectively [46].

Computer modelling of the MMP-26 catalytic domain

The homology modelling structure of the MMP-26 catalytic domain was constructed previously [47] using the SwissModel program [48]. The crystal structure of MMP-12 [33], which exhibits high similarity to MMP-26, was used as a template (PDB accession code 1JK3). Minimization calculations were performed with an Amber forcefield modified to include parameters for zinc and calcium [47]. Both of the putative low-affinity Ca^{2+} ions at the C2 and C3 sites were removed, and the protein structure was minimized to examine the resultant structural changes. The catalytic domain structures of the K189E and V184D mutants were then generated and minimized to investigate any structural changes resulting from these mutations. RMSD (root mean square deviation) values were reported after the comparison of structures.

Cell culture

MDA-MB-231 (A.T.C.C., Manassas, VA, U.S.A.), an established human breast carcinoma cell line, was routinely grown in high-glucose DMEM (Dulbecco's modified Eagle's medium) (Gibco Invitrogen Corporation) supplemented with 10 % (v/v) FBS (fetal bovine serum) (Hyclone), 100 units/ml penicillin and 100 μg/ml streptomycin (Cambrex) in a humidified atmosphere containing 5 % CO_2 at 37 °C.

Transfection of MDA-MB-231 cells and isolation of cell lines expressing wild-type, and K189E and E209A mutant forms of MMP-26

MDA-MB-231 cells were transfected with wild-type, and K189E and E209A mutant forms of MMP-26 containing p3xFLAG-CMV™-13 vectors using Transfectol (GeneChoice). Transfectol-mediated DNA transfections into MDA-MB-231 cells were performed following the instructions provided by GeneChoice. Transfected cell lines were maintained in the presence of 550 μg/ml Geneticin (G-418 sulfate) (Fisher Scientific) and then screened on the basis of FLAG and MMP-26 expression. MMP-26, which was overexpressed from MDA-MB-231 cells, tends to secrete out owing to the signal peptide of the p3x-FLAG vector. Serum-free medium from the cell culture was used for screening colonies. Selected stably transfected cell lines were expanded in the presence of 550 μg/ml G-418 due to rapid loss of vector in the absence of G-418. Cell lines expressing wild-type, and K189E and E209A mutant forms of MMP-26 were analysed for their invasiveness capabilities in modified Boyden chamber (8 μm pore size) (BD Biosciences) invasion assays.

Modified Boyden chamber invasion assays

The invasiveness of MDA-MB-231 cells transfected with wild-type, and K189E and E209A mutant forms of MMP-26 through reconstituted ECM was determined as described previously [9]. Briefly, invasion inserts containing polycarbonate filters with 8 μm pores were coated with 70 μl of 250 μg/ml Type IV collagen (Sigma). The Boyden chambers were dried and sterilized in a laminar flow hood under ultraviolet radiation overnight. To commence the assay, 500 μl of high-glucose DMEM containing 10 % (v/v) FBS was added to the lower chambers, and 300 μl of prepared cell suspensions (1.5×10^5 cells/ml) in Eagle's MEM (minimum essential medium) with or without calcium (Mediatech) was added to each insert for calcium-plus or calcium-minus conditions respectively. In either instance, serum is only present in the medium outside of the invasion inserts. The cells housed inside the invasion inserts have no direct contact with serum at the beginning of the experiment. After 12 h of incubation, invasive cells that had passed through the filter to the lower surface of the membrane were stained using a 0.1 % (w/v) Crystal Violet solution. Cells remaining inside the chamber were removed with a cotton swab, and the filters were removed and mounted on a microscope slide. The membranes were photographed with an Olympus DP10 digital camera under a Nikon FX microscope. Cells were counted by IMA (integrated morphometry analysis). For statistical analyses, the most aggressively invasive cell line, expressing the K189E mutant form of MMP-26, was assumed to reflect 100 % cell invasion. The ratio of the number of invaded cells of each cell lines to the invaded cells of the K189E mutant line was used for subsequent comparative analyses by ANOVA.

RESULTS

Sequence alignment and homology modelling of MMP-26

Crystallographic studies demonstrate that catalytic domains of the MMPs share similar folding topology and metal-binding structures [33]. Thus sequence alignment and homology-modelling structures can be useful tools to predict the calcium-binding sites of MMPs. We used the same sequencing numbering as given by Park et al. [4]. A homology modelling structure of MMP-26 was constructed based on the crystal structure of the catalytic domain of MMP-12 (cdMMP-12) [47]. A comparison of the MMP-26 structure with cdMMP-12 predicted three putative calcium-binding sites, designated C1, C2 and C3 in Figure 1(A). The C1 site of MMP-26 is composed of three side-chain carboxy groups originating from amino acid residues (Asp^{165}, Asp^{188} and Glu^{191}) and three carbonyl groups from the backbone (Gly^{166}, Gly^{168} and Ile^{170}). The C2 site of MMP-26 consists of three carbonyl groups

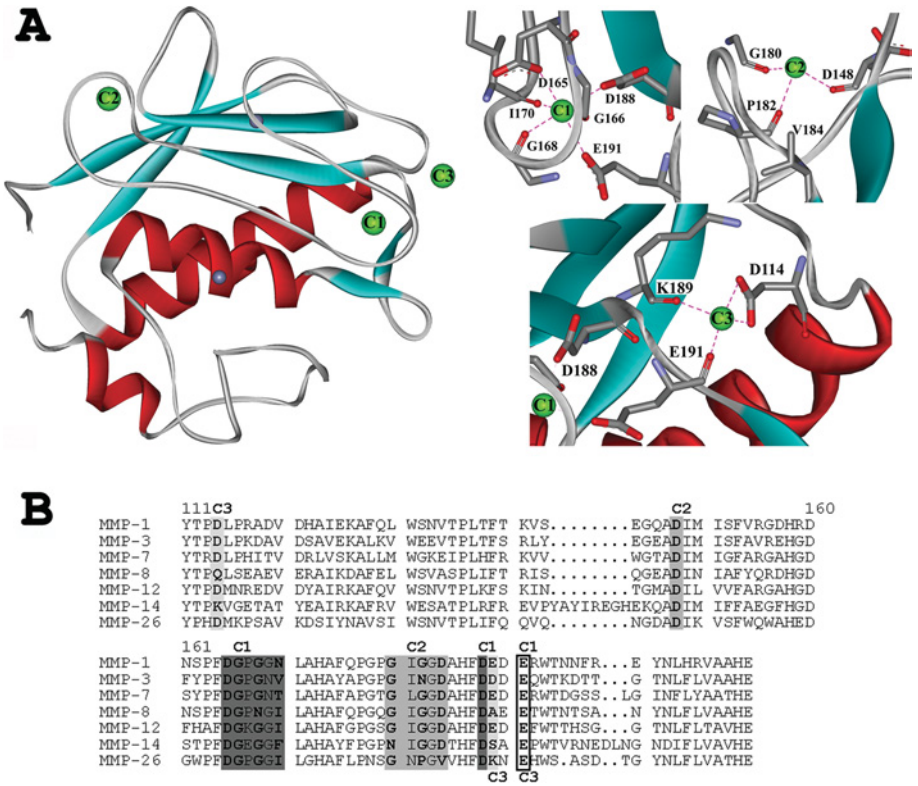

Figure 1 Modelled structure of MMP-26 and sequence alignment data of several MMPs

(**A**) A modelled structure of MMP-26 based on the structure of MMP-12. Green spheres represent Ca^{2+} ions. C1, C2, and C3 represent calcium-binding sites. Small dark blue spheres represent Zn^{2+} ions. Each calcium-binding site is magnified to demonstrate the binding moieties. The RMSD value between the backbones of the minimized and the homology modelled structure of MMP-26 is 1.40 Å. (**B**) Sequence alignment of the MMP26 catalytic domain sequence with the catalytic domains of several MMPs. Conserved calcium-binding residues are boxed. Residues in dark grey correspond to the MMP C1 sites, residues in medium grey correspond to MMP C2 sites, and residues in light grey correspond to MMP C3 sites. Co-ordinating residues, shared by the C1 and C3 sites, are denoted in the black-lined box.

originating from the backbone (Asp^{148}, Gly^{180} and Pro^{182}), which is not feasible for calcium binding. The C3 site is composed of one carboxy group from an amino acid residue (Asp^{114}) and two carbonyl groups from the backbone (Lys^{189} and Glu^{191}).

Sequence alignment of MMP-26 with the available crystallographic structures of other MMPs was used to re-examine the possible ligands at each calcium-binding site (Figure 1B). The possible Ca^{2+} co-ordination at each site for each MMP was summarized (Table 2). Asp^{165}, Gly^{166}, Asp^{188} and Glu^{191} are highly conserved for the C1 site. The calcium at the C1 site is co-ordinated by three carboxy groups and three carbonyl groups. The calcium at the C2 site is co-ordinated by one carboxy group and three carbonyl groups from the backbone with conserved Asp^{148} and Asp^{184}, except in MMP-26 where the latter residue is Val^{184}. The C3 site is the most varied among these sites. The calcium at the C3 site is co-ordinated by two carboxy and two carbonyl groups in MMP-1 [28], MMP-3 [29], MMP-7 [30] and MMP-12 [33] with conserved Asp^{114}, Glu^{189} (Asp^{189} for MMP-3) and Glu^{191} residues. However, the calcium at the C3 site of cdMMP-8 [31] and cdMMP-14 [35] is not found in their crystal structures, perhaps due to the absence of the carboxy group at this site. The calcium at the putative C3 site of MMP-26 is most likely ligated to the carboxy group of Asp^{114} and carbonyl groups of Lys^{189} and Glu^{191}.

Analyses of sequence homology and the modelled MMP-26 structure indicate that cdMMP-26 may contain two possible binding sites with different calcium-binding affinities. The C3 site of MMP-26 may possess modest affinity when compared with the C1 site, while the C2 site may not represent a true calcium-binding site, as these studies predict only three carbonyl groups participating in the possible co-ordination of calcium at this site, analogous to the non-binding C3 sites of cdMMP-8 [31] and cdMMP-14 [35].

Refolding and removal of low-affinity Ca^{2+} ions from recombinant wild-type and mutated forms of MMP-26

Wild-type pro-MMP-26 was auto-activated during folding by dialysis [4,8,40]. Enzymatic activity measurements of the wild-type, and D114A, V184D and K189E mutants showed high rates of fluorescent synthetic peptide hydrolysis, while the D165A and E191A mutants showed very low rates of hydrolysis that were less than 5 % of that seen for wild-type MMP-26. Inactive MMP-26 (E209A), with mutation at the catalytic glutamic acid residue, showed no hydrolysis activity at all. Figure 2 shows that the wild-type MMP-26 preceeded auto-cleavage of the prodomain resulting in one band around 30 kDa (pro-form) and three bands around 20 kDa (activated forms). D114A, V184D and K189E mutations resulted in similar activation patterns. However, D165A and E191A mutants remaining largely intact even show large amounts of precipitation during refolding by dialysis, and mutation at the catalytic glutamic acid residue (E209A) completely abrogated activation (Figure 2).

Removal of low-affinity Ca^{2+} ions by dialysis in the presence of Chelex 100 resulted in a dramatic decreases of catalytic activity for the wild-type and D114A, V184D and K189E mutant forms

Table 2 Comparison of crystal structures of several MMPs

MMP-26 showed one less carboxylic acid residue at both putative low-affinity calcium-binding sites, C2 and C3 with PDB accession codes 1HFC (MMP-1) [28], 1B3D (MMP-3) [29], 1MMQ (MMP-7) [30], 1A86 (MMP-8) [31], 1JK3 (MMP-12) [33], 1BQQ (MT1-MMP) [35]. MMP-8 and MMP-14 show no calcium ion binding at the C3 site, from which Glu^{189} is absent. Likewise, MMP-26 is negative for Glu^{189} at the C3 site. Unlike other MMPs, MMP-26 has Val^{184} instead of aspartic acid.

		Co-ordinating residues		
Name	Calcium co-ordination	C1	C2	C3
MMP-1	Carboxy	Asp^{165}, Asp^{188}, Glu^{191}	Asp^{184}	Asp^{114}, Glu^{189}
	Carbonyl	Gly^{166}, Gly^{168}, Asn^{170}	Asp^{148}, Gly^{180}, Gly^{182}	Glu^{189}, Glu^{191}
			Two water molecules	
MMP-3	Carboxy	Asp^{165}, Asp^{188}, Glu^{191}	Asp^{184}	Asp^{114}, Asp^{189}
	Carbonyl	Gly^{166}, Gly^{168}, Val^{170}	Asp^{148}, Gly^{180}, Asn^{182}	Asp^{189}, Glu^{191}
			Two water molecules	Two water molecules
MMP-7	Carboxy	Asp^{165}, Asp^{188}, Glu^{191}	Asp^{184}	Asp^{114}, Glu^{189}
	Carbonyl	Gly^{166}, Gly^{168}, Thr^{170}	Asp^{148}, Gly^{180}, Gly^{182}	Glu^{189}, Glu^{191}
			Two water molecules	
MMP-8	Carboxy	Asp^{165}, Asp^{188}, Glu^{191}	Asp^{184}	Gln^{114} (amide)
	Carbonyl	Gly^{166}, Asn^{168}, Ile^{170}	Asp^{148}, Gly^{180}, Gly^{182}	Ala^{189}, Glu^{191}
MMP-12	Carboxy	Asp^{165}, Asp^{188}, Glu^{191}	Asp^{184}	Asp^{114}, Glu^{189}
	Carbonyl	Gly^{166}, Gly^{168}, Gly^{170}	Asp^{148}, Gly^{180}, Gly^{182}	Glu^{189}, Glu^{191}
			Two water molecules	Two water molecules
MMP-14	Carboxy	Asp^{165}, Asp^{188}, Glu^{191}	Asp^{184}	Lys^{114} (amide)
	Carbonyl	Gly^{166}, Gly^{168}, Phe^{170}	Asp^{148}, Asn^{180}, Gly^{182}	Ser^{189}, Glu^{191}
MMP-26	Carboxy	Asp^{165}, Asp^{188}, Glu^{191}	Val^{184}	Asp^{114}
	Carbonyl	Gly^{166}, Gly^{168}, Ile^{170}	Asp^{148}, Gly^{180}, Pro^{182}	Lys^{189}, Glu^{191}

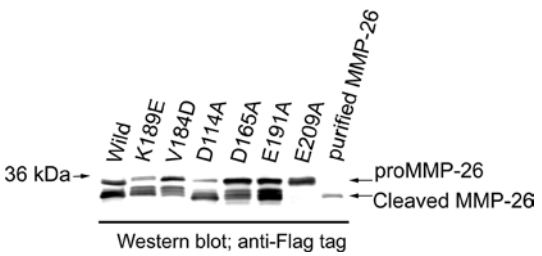

Figure 2 Western blotting of wild-type and mutant forms of MMP-26 after refolding

The pro-form of MMP-26 is slightly less than 36 kDa, while the auto-activated cleavage product is seen at approx. 22 kDa. Only the E209A mutant form is observed as a single band. The cleaved forms of wild-type, and K189E, V184D and D114A mutant forms represent activated MMP-26, although the cleaved forms of D165A and E191A demonstrate less than 5% activity for the fluorescence-quenched substrate hydrolysis, when compared with that of wild-type MMP-26. An anti-FLAG tag antibody was used to detect MMP-26.

of MMP-26. An interesting aspect of the K189E mutant is its higher enzymatic activity than wild-type MMP-26 in the absence of low-affinity Ca^{2+} ions. The activity of LACD-MMP-26 was restored in the presence of 10 mM Ca^{2+} ions within 20 min for the wild-type, and V184D and K189E mutant forms of MMP-26, but the activity of the D114A mutant was not restored (results not shown).

Titration of high-affinity Ca^{2+} ions by Quin2

Quin2 has been utilized to probe high-affinity calcium-binding given its own high affinity ($K_Q = 1.9 \times 10^8$ M^{-1}) for Ca^{2+} ions and the changes in its fluorescent properties after calcium binding [42]. Quin2 fluoresces with an emission maximum at 492 nm, which is far away from that of proteins, and its fluorescence is enhanced approx. 6-fold by the formation of calcium complexes [44]. This fluorescent property of Quin2 can be exploited to calculate the dissociation constants of high-affinity Ca^{2+} ions within the range 0.1 nM–0.1 μM [49].

To determine the true number of high-affinity Ca^{2+} ions in MMP-26, low-affinity Ca^{2+} ions were removed by repeated dialyses as described in the Materials and methods section. When LACD-MMP-26 was titrated with Quin2, the release of the high-affinity Ca^{2+} ion from MMP-26 and formation of the Quin2–Ca^{2+} complex were observed via increases in emission spectra around 490 nm with excitation at 339 nm. Fluorescence intensities at 490 nm following each addition of Quin2 were collected to estimate the total calcium concentration and the dissociation constant of the Quin2–Ca^{2+} complex, $K_{d(QCa)}$ (Figure 3A). Substituting these data into eqn (1) yielded $K_{d(QCa)}$ and the calcium concentration. Application of $K_{d(QCa)}$ and the enzyme concentration to eqn (2) then yielded the calcium-dissociation constant of the enzyme, K_{d1}. The total calcium concentration estimated by these calculations was comparable with the total MMP-26 concentration, $[Ca^{2+}]/[\text{MMP-26}] = 1.4$, with the K_{d1} value of 62.9 nM, which indicated that approximately one high-affinity binding site for calcium exists in MMP-26.

The C2 and C3 residues unique to MMP-26, when compared with other MMPs, were mutated separately to introduce a new carboxy group and enhance Ca^{2+} co-ordination. These mutations facilitated exploration of the possibility of enhanced binding affinity at these sites and thus their possible titration by Quin2. The V184D (C2 site) and K189E (C3 site) mutants yielded K_{d1} values of 63.4 nM and 58.5 nM for the C1 high-affinity Ca^{2+}-binding site respectively, without changing the calcium/enzyme concentration ratio (Table 3). Therefore these mutations at putative low-affinity calcium-binding sites support the presence of a single high-affinity Ca^{2+} ion at the C1 site.

Titration of low-affinity Ca^{2+} ions

LACD-MMP-26 was then titrated with Ca^{2+} ions, and its activity was monitored to estimate the low-affinity calcium-dissociation constant, K_{d2}. To determine the number of low-affinity calcium-binding sites, the K189E and V184D mutants were similarly titrated and monitored. As both mutants contained an additional

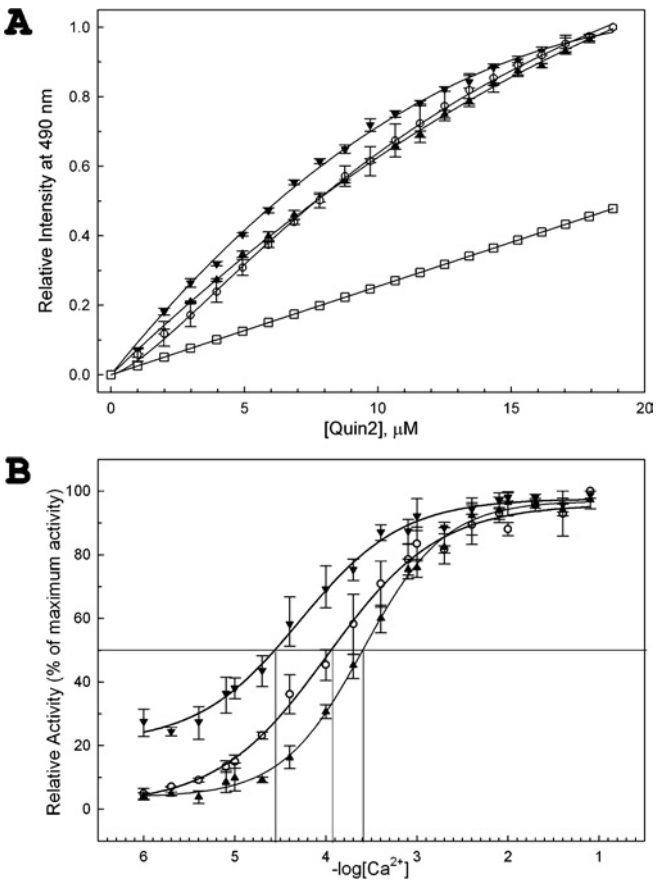

Figure 3 Titration of high- and low-affinity Ca^{2+} ion for measuring calcium-dissociation constants, K_{d1} and K_{d2}

(**A**) Measuring high-affinity calcium-dissociation constant, K_{d1}. Fluorescence intensity of Quin2 binding to Ca^{2+} ions from wild-type, and V184D and K189E mutant form of LACD-MMP-26 at 490 nm. ○, 2.5 μM wild-type LACD-MMP-26; ▲, 2.5 μM V184D mutant form of LACD-MMP-26; ▼, 5 μM K189E mutant form of LACD-MMP-26; □, background Quin-2 spectrum with water or buffer. (**B**) Measuring low-affinity calcium-dissociation constant, K_{d2}. Enzymatic activity was measured by monitoring fluorescence-quenched substrate hydrolysis after incubation with various concentrations of Ca^{2+} ions. LACD-MMP-26 (100 nM) was incubated with various concentrations of Ca^{2+} ions in 0.01 % Brij, 10 mM Hepes/NaOH, pH 7.5, and 10 mM NaCl for 20 min at 25 °C. Maximal activity was taken as 100 %. ○, wild-type MMP-26; ▲, V184D mutant form of LACD-MMP-26; ▼, K189E mutant form of LACD-MMP-26. Approximate negative logarithm values of the low-affinity calcium-dissociation constant for wild-type, and V184D and K189E mutants are 3.93, 3.6 and 4.55 respectively.

Table 3 Calcium dissociation constants

High- and low-affinity calcium dissociation constants, K_{d1} and K_{d2} for wild-type, and V184D and K189E mutant forms of MMP-26.

	Ca^{2+} dissociation constants	
	K_{d1}	K_{d2}
Wild-type	62.9 ± 13.0 nM	0.12 mM
V184D	63.4 ± 16.2 nM	0.24 mM
K189E	62.9 ± 13.0 nM	0.028 mM

carboxy group, either mutation could be expected to result in enhanced calcium-binding affinity. As the calcium concentrations at which 50 % enzymatic activity was observed were much greater than the enzyme concentrations, the necessary assumption for calculations of the low-affinity calcium-dissociation constant, K_{d2}, was satisfied. The resultant K_{d2} value is equal to the EC_{50} value. The K_{d2} values for wild-type, and V184D and K189E mutant forms were 0.12 mM, 0.24 mM and 0.028 mM respectively (Figure 3B and Table 3). The K189E mutant showed increased affinity for Ca^{2+} ions, whereas the V184D mutant showed the opposite result. The K189E mutation caused an approx. 4-fold decrease in the K_{d2} value, whereas the V184D mutation displayed an approx. 2-fold increase in the K_{d2} value when compared with the wild-type. According to the effects of calcium concentration on the activity of the wild-type and mutant forms, the putative C2 low-affinity calcium-binding site, if it exists, did not appear to be involved in enzymatic catalysis, and only a single low-affinity calcium-binding site, C3, affects enzymatic activity.

ANS binding to MMP-26

ANS is a useful indicator of hydrophobic regions in a protein. Used as a fluorescent probe, ANS shows an increase in the quantum yield of fluorescence and a blue shift of the emission spectrum by interaction with the hydrophobic regions in a protein. A common application of ANS is the detection of folding intermediates or unfolded states of protein [50]. In buffer, ANS has little fluorescent intensity, and incubation with tightly folded globular proteins such as carbonic anhydrase, which lacks specific binding sites for ANS, results in no change of the wavelength of maximum fluorescence and intensity. However, incubation with lipid-binding proteins such as apolipoprotein A-I induces an enhancement in ANS fluorescence intensity together with a 35 nm blue shift in its wavelength of maximum emission [50]. Wild-type, and K189E and V184D mutant forms of LACD-MMP-26 were prepared as described in the Materials and methods section. Following the addition of ANS, the formation of ANS–enzyme complexes generated spectra revealing not only an increase in fluorescence intensity, but also blue shifts of the maximum emission peak when compared with background spectra, thereby providing evidence for the existence of hydrophobic areas in MMP-26 (background is shown for wild-type MMP-26, Figure 4A, d). Moreover, conformational changes of enzymes upon binding to Ca^{2+} resulted in increased hydrophobic surface area and a subsequent increase in fluorescence spectra as ANS binds to the enzyme (Figure 4A, a–c). These observations indicated that the hydrophobic regions of MMP-26 accessible to ANS could be altered by the presence or absence of Ca^{2+} ions, which resulted in conformational changes. Monitoring spectra at 480 nm demonstrated a difference in low-affinity calcium effects among the wild-type and mutant forms (Figure 4B). The points of 50 % tertiary structural changes were similar for the K189E and V184D mutant forms compared with wild-type MMP-26 following the addition of Ca^{2+} ions; however, recovery patterns were different. In comparison with wild-type MMP-26, the K189E mutant showed a greater response at low calcium concentrations and smooth changes of its structure, whereas the V184D mutant showed a smaller response at low calcium concentrations and sudden changes of its structure. LACD-MMP-26 was treated with 2 mM EGTA to remove high-affinity Ca^{2+} ion (Figure 4A, d). It revealed that ANS spectra with high-affinity calcium-associated MMP-26 (solid line) are identical with ANS spectra with high-affinity calcium-dissociated MMP-26 (dashed-line), with no changes in fluorescence intensity. This suggested that loss of the high-affinity Ca^{2+} ion did not alter the hydrophobic surface area of MMP-26.

Effects of Ca^{2+} on secondary structure and thermal denaturation by CD spectroscopy

The effects of Ca^{2+} ions on the secondary structure of MMP-26 were explored by measuring CD spectra in the presence or absence of low- and low/high-affinity Ca^{2+} ions. LACD-MMP-26

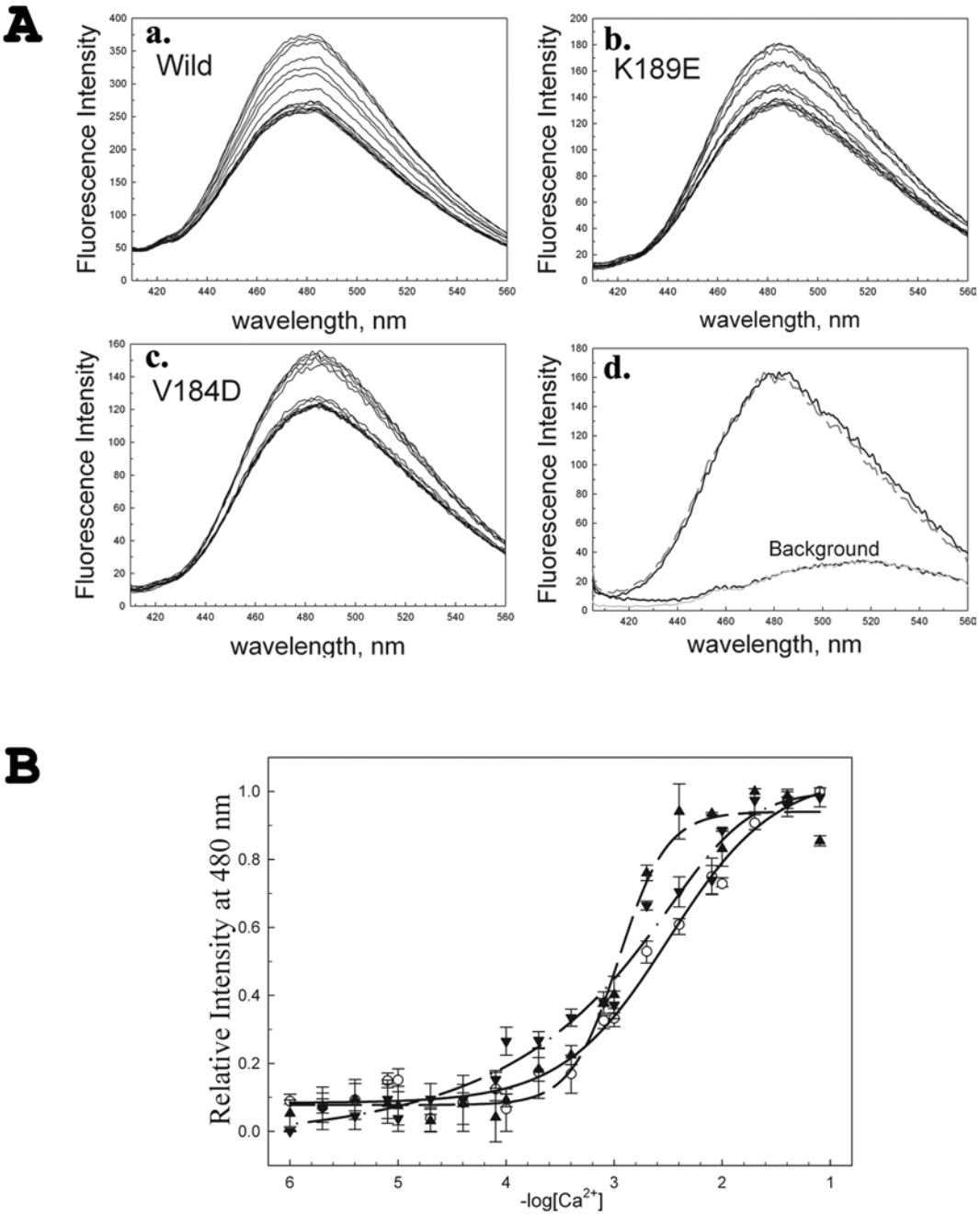

Figure 4 ANS binding to MMP-26; depending on low-affinity Ca^{2+} ions

(**A**) Fluorescence spectra from the mixtures of ANS and protein: 3.4 μM wild-type LACD-MMP-26 and 100 μM ANS in the presence of various concentrations of Ca^{2+} ions (a); 2 μM K189E mutant form of LACD-MMP-26 and 100 μM ANS in the presence of various concentrations of Ca^{2+} ions (b); 2 μM V184D mutant form of LACD-MMP-26 and 100 μM ANS in the presence of various concentrations of a calcium solution (c); 2 μM LACD-MMP-26 and 100 μM ANS before (solid line) or after (broken line) addition of 2 mM EGTA (d). Background spectra were taken from MMP-26 only or ANS only. (**B**) Relative fluorescence intensity at 480 nm. ○ and solid line, wild-type MMP-26; ▲ and dashed line, V184D mutant form of MMP-26; ▼ and dashed-dotted line, K189E mutant form of MMP-26.

was prepared, and then CD spectra were measured with calcium-free buffer (Figure 5A, ●), buffer containing 10 mM EGTA as a Ca^{2+} ion chelator (Figure 5A, ○), or 10 mM $CaCl_2$ (Figure 5A, □). No secondary-structural changes were detected when calcium-associated MMP-26 was compared with calcium-dissociated MMP-26 at 25 °C. To study the effects of Ca^{2+} ions on MMP-26 stability, CD spectra were obtained at 218 nm as increasing temperatures were utilized to induce thermal denaturation. Increased temperature results in an increase of the apparent fractional extent of unfolding, f_{app}, and melting points were measured when f_{app} was 0.5 (Figure 5B). Results showed that the melting points of high-affinity calcium-associated and -dissociated MMP-26 were similar, at 32 and 30 °C respectively. However, the magnitude of the denaturation caused by increased temperature was greater for high-affinity calcium-dissociated MMP-26 (Figure 5B, ○) than for high-affinity calcium-associated MMP-26 (Figure 5B, ●). The 30–32 °C melting temperature range is lower than the known range of melting temperatures for other MMPs [51].

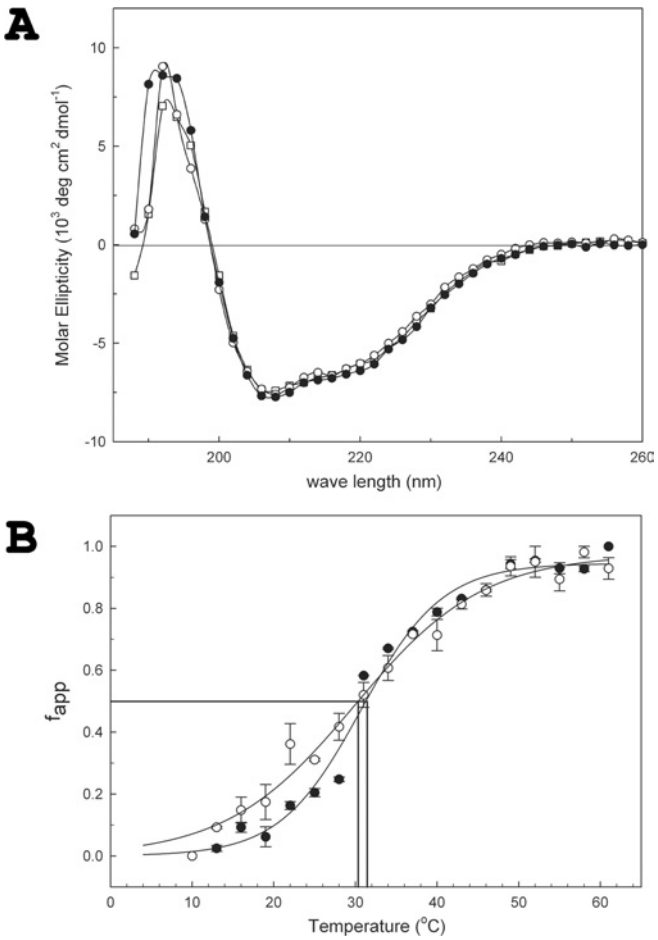

Figure 5 CD spectroscopy of MMP-26 associated or dissociated with calcium binding and thermal denaturation

(**A**) CD spectroscopy of MMP-26 associated or dissociated with Ca^{2+} ion binding. LACD-MMP-26 (5 μM) in 10 mM Tris/HCl, pH 7.5, 10 mM NaCl and 0.01 % Brij-35 (●) was incubated with 2 mM EGTA (○) or 10 mM $CaCl_2$ (□). CD spectroscopy revealed no chages in secondary structure associated or dissociated with Ca^{2+} ion binding. (**B**) Thermal denaturation of LACD-MMP-26 associated or dissociated with high-affinity Ca^{2+} ion binding. ●, 10 μM LACD-MMP-26 dialysed in calcium-free buffer; ○, 10 μM LACD-MMP-26 treated with 2 mM EGTA for 4 h. f_{app} is the apparent fractional extent of unfolding. Melting points for high-affinity calcium-associated and -dissociated LACD-MMP-26 are 32 and 30 °C respectively.

This might be caused by the absence of low-affinity Ca^{2+} ion in MMP-26. Unfortunately, the addition of Ca^{2+} ions resulted in precipitation during the temperature adjustments, and the effects of the low-affinity Ca^{2+} ions against thermal denaturation could not be determined. CD spectroscopy shows that the high-affinity Ca^{2+} ion did not play a pivotal role in stabilizing the secondary structure of MMP-26 at 25 °C and might be involved in the stability of MMP-26 during folding.

Modified Boyden chamber invasion assay

Three stably transfected cell lines expressing wild-type, and K189E and E209A mutant forms of MMP-26 invaded through type IV collagen *in vitro* during cell invasion assays in the presence or absence of Ca^{2+} ions (Figure 6). For the wild-type MMP-26-transfected cell line under calcium-minus conditions there was a significant ($P = 0.001$) decrease in invasion, while the K189E- and E209A-transfected cell lines showed no significant changes in invasive potential ($P = 0.84$ and 0.61 respectively). Thus, while Ca^{2+} ions increased the invasiveness of a wild-type

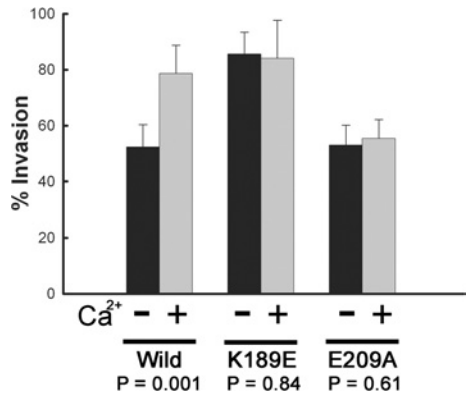

Figure 6 Invasive potential of wild-type, and K189E and E209A mutant forms of MMP-26-transfected cell lines

Invasion assays were performed with modified Boyden chambers, and the percentage of invading cells was quantified as described in the Materials and methods section. Invasion assays were performed under calcium-plus or calcium-minus conditions. Results are means ± S.D. for four separate experiments for each group.

MMP-26-transfected cell line, they failed to alter the invasive potential of either the K189E or E209A MMP-26 mutant-form-transfected cell line. Comparisons of invasiveness between the wild-type MMP-26-transfected cell line under calcium-minus conditions with that of the E209A MMP-26 mutant-form-transfected cell line under calcium-minus or calcium-plus conditions showed insignificant differences ($P = 0.89$ and 0.52 respectively). Comparison of invasiveness between the wild-type MMP-26-transfected cell line under calcium-minus conditions with the K189E MMP-26 mutant-form-transfected cell line showed a significant increase of invasive potential ($P = 0.0002$). Cells transfected with the K189E mutant form demonstrated the high invasive potential in either case, independently of the calcium-plus or calcium-minus conditions.

DISCUSSION

The EC_{50} value of MMP-26 for calcium titration is several hundred times higher than physiological calcium concentrations ranges, which vary from 300 to 1200 nM inside normal cells [26], and therefore normal intracellular conditions serve to maintain MMP-26 in an inactive state. It is when MMP-26 is secreted from the cell or exposed to a transient intracellular calcium influx that it can adopt an active conformation.

When combined with data acquired from inhibition kinetics studies, a previously built MMP-26 homology-modelling structure was useful in predicting the presence of an intermediate-size S_1' pocket at the MMP-26 active site [47]. This MMP-26 structure also revealed a high-affinity calcium-binding site, C1, and putative C2 and C3 low-affinity calcium-binding sites (Figure 1A). The lack of calcium at the analogous C3 site of MMP-8 and MMP-14 as revealed by the crystal structures suggested that carbonyl oxygen atoms alone might not possess sufficient affinity to retain Ca^{2+} ions in the catalytic domain of the MMPs (Figure 1B and Table 2). This suggested further that the C2 site in MMP-26 might not co-ordinate with Ca^{2+} ions. Hence homology modelling and sequence alignment predicted that MMP-26 might have one high-affinity and one low-affinity calcium-binding site at C1 and C3 respectively.

Essential for constructing an enzymatically active structure during the folding of MMP-26 is its ability to bind high-affinity Ca^{2+} ions. Mutations at the C1 site (removal of one carboxylic

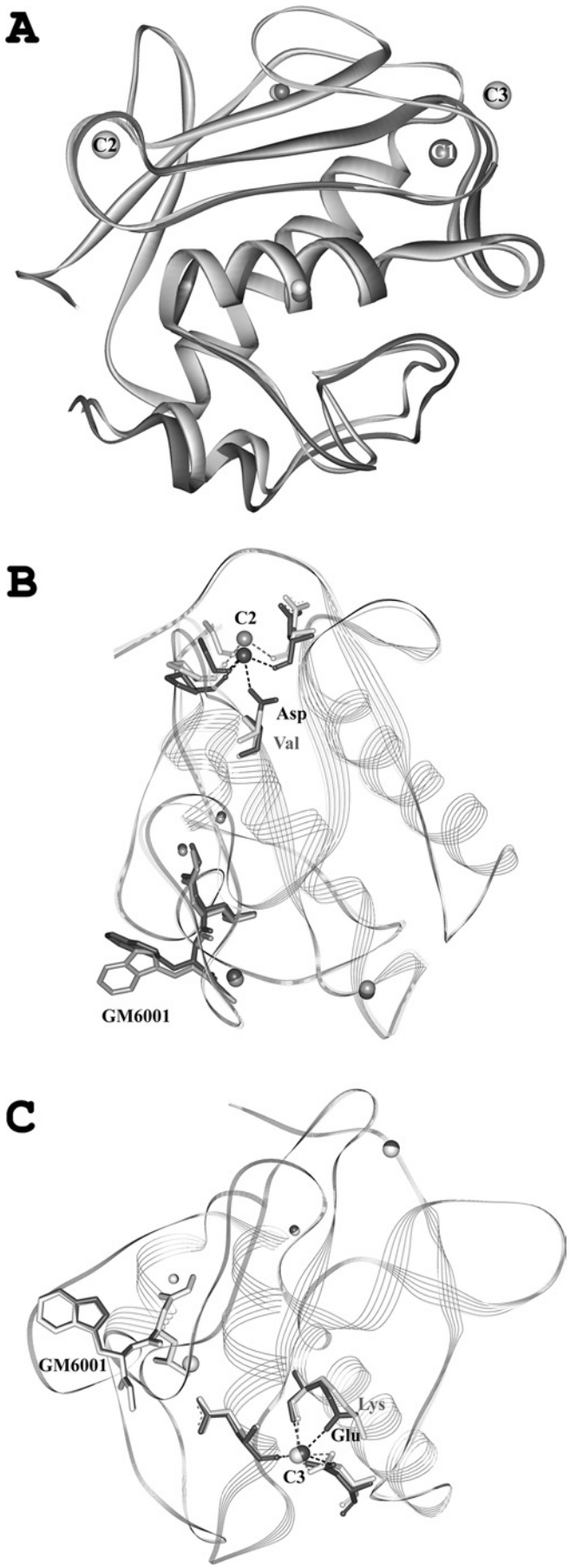

acid ligand, D165A or E191A) resulted in a loss of enzymatic activity using a fluorescence-quenched peptide hydrolysis assay, suggesting that C1 is a true high-affinity calcium-binding site. Quin2 titration of wild-type, and V184D (C2 site) and K189E mutant (C3 site) forms of LACD-MMP-26 supported the presence of a single high-affinity calcium-binding site, C1 (Table 3). Quin2 titration of V184D and K189E mutant forms also suggested that mutations at the putative C2 and C3 low-affinity calcium-binding sites did not generate fluctuations in the high-affinity calcium-binding constant, nor did the addition of a carboxylic acid moiety at these sites fortify calcium affinity at these mutated sites to the levels observed at the high-affinity calcium-binding site. Therefore mutations of the putative low-affinity calcium-binding sites seemed to leave high-affinity calcium binding at the C1 site unaffected. Removal of high-affinity Ca^{2+} ions from LACD-MMP-26 did not induce conformational changes related to the hydrophobic surface area of the protein (Figure 4A, d), nor did it affect the secondary structure (Figure 5A). However, it stabilized secondary structures as observed in thermal denaturation (Figure 5B). Hence, although high-affinity Ca^{2+} ions might be involved in the folding process of MMP-26, apparently they were not essential for maintenance of its secondary structures.

Low-affinity calcium binding to MMP-26 is a reversible and equilibrium state. Low-affinity calcium association and dissociation not only regulated enzymatic activity, but also modulated its tertiary structure, with resultant changes in total hydrophobic surface area. Computer modelling revealed geometric changes at the catalytic site following removal of the low-affinity Ca^{2+} ion, which was actually quite distant from the catalytic site. Figure 7(A) shows the superimposition of two structures with or without the low-affinity Ca^{2+} ions. The elimination of the low-affinity Ca^{2+} ion induced a shift in the active site (small grey spheres at the centre stand for catalytic Zn^{2+} ions). As a result, the structures of the substrate-binding region, and of the catalytic site specifically, were perturbed. Molecular modelling thus supported the assertion that changes at the low-affinity calcium-binding site could result in distortion of the MMP-26 active site.

A mutation at the C2 site (V184D), which adds a carboxylic acid ligand and leads to co-ordinating residues similar to the C2 sites of other MMPs, resulted in an increase in the low-affinity calcium-dissociation constant (K_{d2}, 0.24 mM). Therefore V184D mutation revealed a higher calcium requirement for enzymatic

Figure 7 Modelled structures of MMP-26 with or without low-affinity Ca^{2+} ions, and superimposed structures of wild-type/V184D and wild-type/K189E mutant MMP-26

(**A**) Modelled structure of MMP-26 with or without low-affinity Ca^{2+} ions. The grey solid ribbon structure represents the minimized MMP-26 structure in the presence of low-affinity Ca^{2+} ions, while the dark-grey solid ribbon structure represents that in the absence of these ions resulting in LACD-MMP-26. The large grey spheres, which were designated C2 and C3 and were eliminated for further minimization, are putative low-affinity Ca^{2+} ions. The dark-grey sphere, designated C1, is a high-affinity Ca^{2+} ion. Small grey and dark-grey spheres at the centre of MMP-26 are the catalytic Zn^{2+} ions before and after elimination of the low-affinity Ca^{2+} ions respectively. Small grey and dark-grey spheres at the top of MMP-26 are the structural Zn^{2+} ions. The RMSD value between the backbones of the wild-type and LACD-MMP-26 structure is 1.23 Å. (**B**) Superimposition of the wild-type and V184D mutant MMP-26 structures. The grey ribbon structure represents the minimized structure of wild-type MMP-26 and the black ribbon structure represents the minimized structure of the MMP-26 mutant forms. The inhibitor, GM6001, is bound to the catalytic site of MMP-26. The V184D mutation alters both the C2 site and the active site of MMP-26 when compared with wild-type MMP-26, resulting in a perturbed orientation of the bound inhibitor. The RMSD value between the backbones of the wild-type and V184D mutant MMP-26 structure is 0.56 Å. (**C**) Superimposed structure of wild-type/K189E mutant MMP-26. Protein representation follows the same way of V184D mutant representation above. The K189E mutation does not alter the C3 site or the active site of MMP-26 when compared with the wild-type, and there is no change in orientation of the bound inhibitor (GM6001). The RMSD value between the backbones of the wild-type and K189E mutant MMP-26 structure is 0.15 Å.

activity when compared with wild-type MMP-26. ANS spectra revealed that the calcium concentrations at which tertiary structural changes within the V184D mutant were first induced is higher than that for wild-type MMP-26, but this resistance to change was overcome in the presence of additional Ca^{2+} ions. This might be the result of competition between the C3 and artificial C2 sites for Ca^{2+} ions following this mutation. Molecular modelling of the V184D mutant showed that the introduction of a carboxylic acid moiety (Asp^{184}) at the C2 site might initiate calcium binding with subsequent changes at the C2 site and the catalytic site of MMP-26, resulting in a new binding orientation for the inhibitor, GM6001 (Figure 7B). Because the C2 and C3 sites share the same β-sheet as the artificial Asp^{184} residue, these sites are co-operative. Therefore calcium binding at the C2 site in the absence of calcium binding at the C3 site might increase perturbation of the catalytic site, which persisted until calcium binding at the C3 site relieves this distortion. This structural distortion might be the reason that calcium-binding affinity enforcement at the C2 site by the additional Ca^{2+} co-ordinate (Asp^{184}) increases the Ca^{2+} requirement for enzymatic activity and rapid tertiary structural changes induced by calcium binding. These data combined with sequence analysis suggest that C2 is not a true low-affinity calcium-binding site.

D114A mutation at the C3 site resulted in irreversible loss of enzymatic activity triggered by low-affinity calcium-binding. As long as Ca^{2+} ions were present during folding, the D114A mutant form of MMP-26 retained enzymatic activity, but once the Ca^{2+} ions were removed, enzymatic activity could not be recovered even if the Ca^{2+} ions were restored. K189E mutation at the C3 site resulted in a decrease of the low-affinity calcium-dissociation constant (K_{d2}, 0.028 mM). Therefore a K189E mutation at C3 site revealed a lower Ca^{2+} requirement for enzymatic activity compared with the wild-type. Moreover ANS-binding spectra showed that the tertiary structure of the K89E mutant changed initially at lower calcium concentrations than that for wild-type MMP-26. Therefore the K189E mutation successfully fortified calcium-binding affinity at C3 site. According to molecular modelling of the K189E mutant, addition of a carboxylic acid moiety (from Glu^{189}) by mutation did not alter either the C3 calcium-binding site or the catalytic site of MMP-26, resulting in no change in orientation of the inhibitor, GM6001. Nevertheless, the addition of the Ca^{2+} co-ordinate (Glu^{189}) at the C3 site did result in enhanced calcium binding (Figure 7C).

Results of the invasion assays corresponded to the kinetics data. As the E209A mutation resulted in a loss of enzymatic activity owing to mutation of the catalytic Glu^{209}, a cell line transfected with the E209A mutant form of MMP-26 showed that decreased invasive potential was independent of Ca^{2+} ions, resulting in an invasive potential similar to that of the wild-type MMP-26-transfected cell line under calcium-minus conditions. As Ca^{2+} ions restored enzymatic activity for wild-type MMP-26, Ca^{2+} ions also increased the invasive potential of the wild-type MMP-26-transfected cell line, but this was not true for the E209A-transfected cell line. In contrast with these findings, cells transfected with the K189E mutant form of MMP-26 showed a high invasive potential that was independent of Ca^{2+} ions.

In summary, MMP-26 has one high-affinity calcium-binding site, designated here as C1, and one low-affinity calcium-binding site, designated C3, with 62.9 nM and 120 μM dissociation constants respectively. High-affinity Ca^{2+} ion binding stabilizes secondary-structural features during folding, whereas low-affinity Ca^{2+} ion binding serves to regulate enzymatic activity through changes in enzyme tertiary structure. The D165A or E191A mutations at the C1 site show a loss of enzymatic function, while the D114A mutation at the C3 site demonstrates an irreversible loss of enzymatic function triggered by low-affinity calcium binding. The K189E mutation at C3 showed lower calcium requirements for regulation of enzymatic activity and changes in tertiary structure when compared with wild-type MMP-26, whereas the V184D mutation at the C2 site showed opposite effects. Invasion assays support a role for Ca^{2+} ions in the regulation of ECM degradation and cell invasion. These results suggest that the enzymatic activity of MMP-26 might be regulated by calcium concentrations in cellular systems.

This work was supported in part by grants from the Susan G. Komen Breast Cancer Foundation, Elsa U. Pardee Foundation, and DOD (Department of Defense) Congressionally Directed Medical Research Program DMAD17-02-1-238, a Developing Scholar Award and a Program Enhancement Grant from Florida State University (to Q.-X. A. S.), and a Postdoctoral Research Fellowship from the American Heart Association AHA0225324B (to H. I. P.). We appreciate Robert G. Newcomer at the laboratory of Q.-X. A. S. for pre-submission editorial review and revisions, and Dr Ewa Anna Bienkiewicz at the Biomedical Proteomics Laboratory at Florida State University for excellent technical assistance with CD experiments.

REFERENCES

1 Mott, J. D. and Werb, Z. (2004) Regulation of matrix biology by matrix metalloproteinases. Curr. Opin. Cell Biol. **16**, 558–564
2 DeClerck, Y. A., Mercurio, A. M., Stack, M. S., Chapman, H. A., Zutter, M. M., Muschel, R. J., Raz, A., Matrisian, L. M., Sloane, B. F., Noel, A. et al. (2004) Proteases, extracellular matrix, and cancer: a workshop of the path B study section. Am. J. Pathol. **164**, 1131–1139
3 Nagase, H., Visse, R. and Murphy, G. (2006) Structure and function of matrix metalloproteinases and TIMPs. Cardiovasc. Res. **69**, 562–573
4 Park, H. I., Ni, J., Gerkema, F. E., Liu, D., Belozerov, V. E. and Sang, Q.-X. (2000) Identification and characterization of human endometase (matrix metalloproteinase-26) from endometrial tumor. J. Biol. Chem. **275**, 20540–20544
5 de Coignac, A. B., Elson, G., Delneste, Y., Magistrelli, G., Jeannin, P., Aubry, J. P., Berthier, O., Schmitt, D., Bonnefoy, J. Y. and Gauchat, J. F. (2000) Cloning of MMP-26: a novel matrilysin-like proteinase. Eur. J. Biochem. **267**, 3323–3329
6 Uria, J. A. and Lopez-Otin, C. (2000) Matrilysin-2, a new matrix metalloproteinase expressed in human tumors and showing the minimal domain organization required for secretion, latency, and activity. Cancer Res. **60**, 4745–4751
7 Marchenko, G. N., Ratnikov, B. I., Rozanov, D. V., Godzik, A., Deryugina, E. I. and Strongin, A. Y. (2001) Characterization of matrix metalloproteinase-26, a novel metalloproteinase widely expressed in cancer cells of epithelial origin. Biochem. J. **356**, 705–718
8 Park, H. I., Turk, B. E., Gerkema, F. E., Cantley, L. C. and Sang, Q.-X. (2002) Peptide substrate specificities and protein cleavage sites of human endometase/matrilysin-2/matrix metalloproteinase-26. J. Biol. Chem. **277**, 35168–35175
9 Zhao, Y. G., Xiao, A. Z., Newcomer, R. G., Park, H. I., Kang, T., Chung, L. W., Swanson, M. G., Zhau, H. E., Kurhanewicz, J. and Sang, Q.-X. (2003) Activation of pro-gelatinase B by endometase/matrilysin-2 promotes invasion of human prostate cancer cells. J. Biol. Chem. **278**, 15056–15064
10 Savinov, A. Y., Remacle, A. G., Golubkov, V. S., Krajewska, M., Kennedy, S., Duffy, M. J., Rozanov, D. V., Krajewski, S. and Strongin, A. Y. (2006) Matrix metalloproteinase 26 proteolysis of the NH_2-terminal domain of the estrogen receptor β correlates with the survival of breast cancer patients. Cancer Res. **66**, 2716–2724
11 Zhao, Y. G., Xiao, A. Z., Park, H. I., Newcomer, R. G., Yan, M., Man, Y. G., Heffelfinger, S. C. and Sang, Q.-X. (2004) Endometase/matrilysin-2 in human breast ductal carcinoma in situ and its inhibition by tissue inhibitors of metalloproteinases-2 and -4: a putative role in the initiation of breast cancer invasion. Cancer Res. **64**, 590–598
12 Lee, S., Desai, K. K., Iczkowski, K. A., Newcomer, R. G., Wu, K. J., Zhao, Y. G., Tan, W. W., Roycik, M. D. and Sang, Q.-X. (2006) Coordinated peak expression of MMP-26 and TIMP-4 in preinvasive human prostate tumor. Cell Res. **16**, 750–758
13 Ahokas, K., Skoog, T., Suomela, S., Jeskanen, L., Impola, U., Isaka, K. and Saarialho-Kere, U. (2005) Matrilysin-2 (matrix metalloproteinase-26) is upregulated in keratinocytes during wound repair and early skin carcinogenesis. J. Invest. Dermatol. **124**, 849–856
14 Kahl, C. R. and Means, A. R. (2003) Regulation of cell cycle progression by calcium/calmodulin-dependent pathways. Endocr. Rev. **24**, 719–736
15 Carafoli, E., Santella, L., Branca, D. and Brini, M. (2001) Generation, control, and processing of cellular calcium signals. Crit. Rev. Biochem. Mol. Biol. **36**, 107–260
16 Kohn, E. C., Alessandro, R., Spoonster, J., Wersto, R. P. and Liotta, L. A. (1995) Angiogenesis: role of calcium-mediated signal transduction. Proc. Natl. Acad. Sci. U.S.A. **92**, 1307–1311

17 Berridge, M. J., Bootman, M. D. and Lipp, P. (1998) Calcium: a life and death signal. Nature **395**, 645–648
18 Sergeev, I. N. (2005) Calcium signaling in cancer and vitamin D. J. Steroid Biochem. Mol. Biol. **97**, 145–151
19 Sorimachi, H., Ishiura, S. and Suzuki, K. (1997) Structure and physiological function of calpains. Biochem. J. **328**, 721–732
20 Hosfield, C. M., Elce, J. S., Davies, P. L. and Jia, Z. (1999) Crystal structure of calpain reveals the structural basis for Ca^{2+}-dependent protease activity and a novel mode of enzyme activation. EMBO J. **18**, 6880–6889
21 Berridge, M. J., Bootman, M. D. and Roderick, H. L. (2003) Calcium signalling: dynamics, homeostasis and remodelling. Nat. Rev. Mol. Cell Biol. **4**, 517–529
22 Cook, S. J. and Lockyer, P. J. (2006) Recent advances in Ca^{2+}-dependent Ras regulation and cell proliferation. Cell Calcium **39**, 101–112
23 Albert, B., Bray, D., Lewis, J., Raff, M., Roberts, K. and Watson, J. D. (1994) Molecular Biology of the Cell, 3rd edn, Garland Publishing, New York
24 Strobl, S., Fernandez-Catalan, C., Braun, M., Huber, R., Masumoto, H., Nakagawa, K., Irie, A., Sorimachi, H., Bourenkow, G., Bartunik, H. et al. (2000) The crystal structure of calcium-free human m-calpain suggests an electrostatic switch mechanism for activation by calcium. Proc. Natl. Acad. Sci. U.S.A. **97**, 588–592
25 Lowry, C. L., McGeehan, G. and Le Vine, III, H. (1992) Metal ion stabilization of the conformation of a recombinant 19-kDa catalytic fragment of human fibroblast collagenase. Proteins **12**, 42–48
26 Prasad, A. and Pedigo, S. (2005) Calcium-dependent stability studies of domains 1 and 2 of epithelial cadherin. Biochemistry **44**, 13692–13701
27 Averna, M., Stifanese, R., De Tullio, R., Defranchi, E., Salamino, F., Melloni, E. and Pontremoli, S. (2006) Interaction between catalytically inactive calpain and calpastatin: evidence for its occurrence in stimulated cells. FEBS J. **273**, 1660–1668
28 Spurlino, J. C., Smallwood, A. M., Carlton, D. D., Banks, T. M., Vavra, K. J., Johnson, J. S., Cook, E. R., Falvo, J., Wahl, R. C., Pulvino, T. A. et al. (1994) 1.56 Å structure of mature truncated human fibroblast collagenase. Proteins **19**, 98–109
29 Chen, L., Rydel, T. J., Gu, F., Dunaway, C. M., Pikul, S., Dunham, K. M. and Barnett, B. L. (1999) Crystal structure of the stromelysin catalytic domain at 2.0 Å resolution: inhibitor-induced conformational changes. J. Mol. Biol. **293**, 545–557
30 Browner, M. F., Smith, W. W. and Castelhano, A. L. (1995) Matrilysin–inhibitor complexes: common themes among metalloproteases. Biochemistry **34**, 6602–6610
31 Brandstetter, H., Engh, R. A., von Roedern, E. G., Moroder, L., Huber, R., Bode, W. and Grams, F. (1998) Structure of malonic acid-based inhibitors bound to human neutrophil collagenase: a new binding mode explains apparently anomalous data. Protein Sci. **7**, 1303–1309
32 Gall, A. L., Ruff, M., Kannan, R., Cuniasse, P., Yiotakis, A., Dive, V., Rio, M. C., Basset, P. and Moras, D. (2001) Crystal structure of the stromelysin-3 (MMP-11) catalytic domain complexed with a phosphinic inhibitor mimicking the transition state. J. Mol. Biol. **307**, 577–586
33 Lang, R., Kocourek, A., Braun, M., Tschesche, H., Huber, R., Bode, W. and Maskos, K. (2001) Substrate specificity determinants of human macrophage elastase (MMP-12) based on the 1.1 Å crystal structure. J. Mol. Biol. **312**, 731–742
34 Moy, F. J., Chanda, P. K., Chen, J. M., Cosmi, S., Edris, W., Levin, J. I. and Powers, R. (2000) High-resolution solution structure of the catalytic fragment of human collagenase-3 (MMP-13) complexed with a hydroxamic acid inhibitor. J. Mol. Biol. **302**, 671–689
35 Fernandez-Catalan, C., Bode, W., Huber, R., Turk, D., Calvete, J. J., Lichte, A., Tschesche, H. and Maskos, K. (1998) Crystal structure of the complex formed by the membrane type 1-matrix metalloproteinase with the tissue inhibitor of metalloproteinases-2, the soluble progelatinase A receptor. EMBO J. **17**, 5238–5248
36 Kohn, E., Jacobs, W., Kim, Y. S., Alessandro, R., Stetler-Stevenson, W. G. and Liotta, L. A. (1994) Calcium influx modulates expression of matrix metalloproteinase-2 (72-kDa type IV collagenase, gelatinase A). J. Biol. Chem. **269**, 21505–21511
37 Housley, T. J., Baumann, A. P., Braun, I. D., Davis, G., Seperack, P. K. and Wilhelm, S. M. (1993) Recombinant Chinese hamster ovary cell matrix metalloprotease-3 (MMP-3, stromelysin-1): role of calcium in promatrix metalloprotease-3 (pro-MMP-3, prostromelysin-1) activation and thermostability of the low mass catalytic domain of MMP-3. J. Biol. Chem. **268**, 4481–4487
38 Winberg, J.-O., Berg, E., Kolset, S. O. and Uhlin-Hansen, L. (2003) Calcium-induced activation and truncation of promatrix metalloproteinase-9 linked to the core protein of chondroitin sulfate proteoglycans. Eur. J. Biochem. **270**, 3996–4007
39 Yu, M., Sato, H., Seiki, M., Spiegel, S. and Thompson, E. W. (1997) Calcium influx inhibits MT1-MMP processing and blocks MMP-2 activation. FEBS Lett. **412**, 568–572
40 Marchenko, N. D., Marchenko, G. N. and Strongin, A. Y. (2002) Unconventional activation mechanisms of MMP-26, a human matrix metalloproteinase with a unique PHCGXXD cysteine-switch motif. J. Biol. Chem. **277**, 18967–18972
41 Blinks, J. R. (1989) Use of calcium-regulated photoproteins as intracellular Ca^{2+} indicators. Methods Enzymol. **172**, 164–203
42 Hartleib, J., Geschwindner, S., Scharff, E. I. and Ruterjans, H. (2001) Role of calcium ions in the structure and function of the di-isopropylfluorophosphatase from *Loligo vulgaris*. Biochem. J. **353**, 579–589
43 Linse, S., Helmersson, A. and Forsen, S. (1991) Calcium binding to calmodulin and its globular domains. J. Biol. Chem. **266**, 8050–8054
44 Bryant, D. T. (1985) Quin 2: the dissociation constants of its Ca^{2+} and Mg^{2+} complexes and its use in a fluorimetric method for determining the dissociation of Ca^{2+}–protein complexes. Biochem J. **226**, 613–616
45 Weber, G. and Young, L. B. (1964) Fragmentation of bovine serum albumin by pepsin. I. The origin of the acid expansion of the albumin molecule. J. Biol. Chem. **239**, 1415–1423
46 Kuwajima, K (1995) Circular dichroism. In Protein Stability and Folding: Theory and Practice (Shirley, B. A., ed.), pp. 115–135, Humana Press, Totawa
47 Park, H. I., Jin, Y., Hurst, D. R., Monroe, C. A., Lee, S., Schwartz, M. A. and Sang, Q.-X. (2003) The intermediate S1′ pocket of the endometase/matrilysin-2 active site revealed by enzyme inhibition kinetic studies, protein sequence analyses, and homology modeling. J. Biol. Chem. **278**, 51646–51653
48 Schwede, T., Kopp, J., Guex, N. and Peitsch, M. C. (2003) SWISS-MODEL: an automated protein homology-modeling server. Nucleic Acids Res. **31**, 3381–3385
49 Stenberg, Y., Linse, S., Drakenberg, T. and Stenflo, J. (1997) The high affinity calcium-binding sites in the epidermal growth factor module region of vitamin K-dependent protein S. J. Biol. Chem. **272**, 23255–23260
50 Rogers, D. P., Brouillette, C. G., Engler, J. A., Tendian, S. W., Roberts, L., Mishra, V. K., Anantharamaiah, G. M., Lund-Katz, S., Phillips, M. C. and Ray, M. J. (1997) Truncation of the amino terminus of human apolipoprotein A-I substantially alters only the lipid-free conformation. Biochemistry **36**, 288–300
51 Tordai, H. and Patthy, L. (1999) The gelatin-binding site of the second type-II domain of gelatinase A/MMP-2. Eur. J. Biochem. **259**, 513–518

Received 11 September 2006/27 November 2006; accepted 18 December 2006
Published as BJ Immediate Publication 18 December 2006, doi:10.1042/BJ20061390